Gastro Hep Advances 2022;1:461–470

ORIGINAL RESEARCH—BASIC

Regulatory T Cell (Treg) Cytotoxic T Lymphocyte–associated Antigen-4 Deficits in Biliary Atresia (BA) and Disease Rescue With Treg Augmentation in Murine BA

Yuhuan Luo,[1] Joseph Bednarek,[2] Alexander Chaidez,[1] Shaikh Atif,[3] Dong Wang,[4] and Cara L. Mack[1]

[1]Section of Gastroenterology, Hepatology & Nutrition, Department of Pediatrics, Children's Hospital Colorado, University of Colorado School of Medicine. Aurora, Colorado, [2]Department of Pathology, University of Utah. Salt Lake City, Utah, [3]Division of Allergy & Immunology, Department of Medicine, University of Colorado School of Medicine. Aurora, Colorado, and [4]University of Colorado School of Medicine. Aurora, Colorado

BACKGROUND AND AIMS: Biliary atresia (BA) entails an inflammatory injury of the biliary tree, leading to fibrosis of the extrahepatic and intrahepatic bile ducts. The chronic inflammatory biliary injury may be due to lack of appropriate regulatory T cell (Treg) suppression of inflammation. The aims of the study were to characterize Treg deficits in human BA and to determine if Treg augmentation therapy improved outcomes in the rhesus rotavirus (RRV)–induced mouse model of BA. **METHODS:** Immunophenotyping of human peripheral blood and liver Tregs was performed with flow cytometry, Vectra-6 multicolor immunohistochemistry (IHC), and real-time polymerase chain reaction. Measured outcomes of Treg augmentation with the interleukin-2 monoclonal antibody JES6-1/interleukin-2 in the RRV-induced mouse model of BA included survival, direct bilirubin, IHC, and liver flow cytometry. **RESULTS:** Patients with BA had decreased peripheral blood Treg frequency and lack of cytotoxic T lymphocyte–associated antigen-4 (CTLA-4) upregulation despite a highly activated, effector Treg phenotype. IHC revealed decreased liver Treg frequency and Treg CTLA-4 expression. Treg augmentation in the murine model led to increased survival, decreased direct bilirubin levels and liver inflammation, and expansion of resident macrophages. In addition to the M2 phenotype of resident macrophages, these cells adopted an inflammatory M1 phenotype in response to RRV infection, which was inhibited with Treg augmentation. **CONCLUSION:** Patients with BA have Treg deficiencies associated with lack of sufficient CTLA-4 expression that is necessary for cell-cell contact inhibition of inflammatory responses. Treg augmentation therapy in murine BA protected from disease. Future treatment trials for BA should include agents that enhance Treg number or function, mimic CTLA-4 function, and promote anti-inflammatory M2 macrophage phenotypes.

Keywords: Bile Duct; Children; Cholestasis; Cytotoxic T Lymphocyte–associated Antigen-4; Forkhead Box P3

Biliary atresia (BA) is a puzzling cause of neonatal cholestasis that entails an inflammatory injury of the biliary tree, leading to fibrosis of both the extrahepatic and intrahepatic bile ducts.[1] At the time of diagnosis, the extrahepatic fibrotic biliary remnant is removed, and a Kasai portoenterostomy is performed in an attempt to re-establish bile flow. Despite this surgical intervention, the intrahepatic bile duct injury ensues, leading to cirrhosis and the need for liver transplantation in the majority. Only ~25% of children with BA will enter adulthood with their native liver, and most of these patients have evidence of cirrhosis.[2] A critical barrier to progress in treating BA is the lack of a definitive cause for this destructive biliary disease.

Adaptive and innate immune responses are activated in BA;[3–11] however, the cause of these exaggerated immune responses is poorly understood. The chronic inflammatory attack on the biliary system may be due to lack of appropriate suppression of inflammation in the setting of dysfunctional regulatory T cells (Tregs). The Treg subset of human $CD4^+$ T cells ($CD25^{hi}$, $CD127^{lo}$, and transcription factor forkhead box P3 [$FOXP3^+$]) is responsible for controlling immune responses to prevent "bystander damage" of healthy tissue and for preventing activation of autoreactivity.[12] Previous studies have shown that Treg deficiencies were associated with autoreactive T cells targeting bile duct epithelia in the rhesus rotavirus (RRV)–induced mouse model of BA.[13–15] Adoptive transfer of purified adult Tregs into BA mice prevented biliary obstruction and increased survival, suggesting that BA Tregs were dysfunctional and unable to control inflammation.[13,14] In human BA, decreased frequencies of peripheral blood and liver Tregs have been described,[16,17] and lower levels of circulating Tregs were associated with poor outcomes.[18] The aims of

Abbreviations used in this paper: **BA, biliary atresia; BSS, balanced salt solution; CTLA-4, cytotoxic T lymphocyte–associated antigen-4; DOL, day of life; FOXP3, forkhead box P3; IHC, immunohistochemistry; PBMCs, peripheral blood mononuclear cells; RRV, rhesus rotavirus; Treg, regulatory T cell.**

Most current article

2772-5723
https://doi.org/10.1016/j.gastha.2021.12.012

the present study were twofold: (1) to determine if there were functional deficits in human BA Tregs based on changes in regulatory molecules and (2) to determine if Treg augmentation therapy improved outcomes in the RRV-induced mouse model of BA.

Results

Activated Circulating Tregs Lack Upregulation of Suppressive Molecules in BA

Peripheral blood mononuclear cells (PBMCs) were obtained at the time of liver transplantation in BA (N = 21) and at the time of liver biopsy or transplant for other liver disease controls (N = 19: Alagille syndrome, N = 5; nonalcoholic fatty liver disease, N = 6; genetic/metabolic, N = 3; other, N = 5). The mean age ± standard deviation at the time of blood collection was 4.79 ± 5.29 years in BA and 8.2 ± 6.61 years in other liver disease controls ($P = .078$). The aim of the flow cytometry studies was to determine key Treg constituents that may be altered in BA, including (1) Treg maturation subsets, (2) activation markers and suppressive molecules necessary for cell-cell contact inhibition, and (3) chemokine receptors necessary for Treg trafficking to the liver (Figure 1A). Tregs were characterized based on $CD3^+CD4^+FOXP3^+CD25^+CD127^-$ cellular expression (Figure 1B). The percentage of circulating Tregs was significantly decreased in BA compared with controls (Figure 1C). BA Tregs displayed an activated phenotype based on increased expression of activation markers CD69 and CD38 (Figure 1C). Treg subsets were also significantly different in BA and controls, with lower frequencies of naïve and central memory Tregs and increased frequencies of effector memory and terminally differentiated Tregs in BA (Figure 1D). Despite the activated Treg status in BA, there was lack of significant increases in the frequency of Tregs expressing suppressive molecules cytotoxic T lymphocyte–associated antigen-4 (CTLA-4) and galectin 1; only LAG3 increased in BA (Figure 2E). Analysis of Treg chemokine receptors necessary for honing to the liver revealed that BA Tregs had increased expression of all chemokine receptors compared with controls (Figure 2F), suggesting chemokine-induced trafficking to the liver. Similar trends were found with analysis of the mean fluorescent intensity of the various surface markers (Figure A1). Cytokines produced by Tregs that function to inhibit inflammation were assessed by real-time polymerase chain reaction (PCR) of purified PBMC Tregs. No differences in mRNA levels of transforming growth factor beta (*TGF-β*), interleukin-10, and inducible costimulator between groups were identified (Figure A2).

Deficits in Treg Frequency and CTLA-4 Expression in Livers of Patients With BA

To determine if the observed Treg deficits in peripheral blood were also found in liver tissue, Vectra-6 immunohistochemistry (IHC) was performed, whereby multiple constituents of Tregs could be visualized within a single tissue sample (Figure 2A). Liver tissue samples at the time of diagnosis of BA (N = 10) or other liver disease controls were assessed (N = 10: Alagille syndrome, N = 2; endocrinopathy with cholestasis, N = 2; parenteral nutrition–associated cholestasis, N = 2; PFIC2, N = 1; other cholestasis, N = 3) (age: BA: 0.13 ± 0.05 years; controls: 0.18 ± 0.05 years). Increased frequencies of portal tract $CD3^+$ T cells and decreased frequencies of Tregs ($CD3^+FOXP3^+$ T cells) and CTLA-4^+ Tregs were observed in BA livers compared with controls (Figure 2B). Importantly, the BA Tregs had decreased mean intensity and total weight of CTLA-4 Treg expression compared with controls (Figure 2C and Figure A3), suggesting deficits in CTLA-4–driven cell-cell contact suppressive function. In addition, the total weight of LAG3 per Treg was significantly decreased in BA portal tracts; however, there was no difference in the Treg LAG3 mean intensity between groups (Figure 2C and Figure A3).

Treg Augmentation Therapy Rescues From Disease in the RRV-induced Mouse Model of BA

Based on the observed findings of Treg deficits in human BA, the impact of Treg enhancement in the mouse model of BA was assessed. Previous studies have shown that in vivo induction of Tregs with an interleukin-2 (IL-2) monoclonal antibody (JES6-1) + IL-2 led to increased numbers and enhanced function of Tregs, associated with protection from autoimmunity.[19,20] Newborn mouse pups were given a single injection of RRV or balanced salt solution (BSS) (controls) on day of life (DOL) 1, followed by injections of either JES6-1/IL-2 or isotype control on DOL 4, 5, and 6 for RRV-infected mice; mice were sacrificed on DOL 14. Significant improvement in survival (Figure 3A) and decreased biliary obstruction, shown by diminished direct bilirubin levels (Figure 3B) and patency of the extrahepatic duct (Figure 3C and Figure A4), was observed in the RRV-infected mice that received JES6-1/IL-2. Within the liver, RRV-infected BA mice had decreased frequencies of Tregs compared with BSS controls, and the Treg frequency significantly increased in the JES6-1/IL-2–treated mice (Figure 4A). Similar to the liver immune profile in human BA, the RRV-infected BA mice had significantly increased liver infiltrates of many immune cell subtypes, including B cells, $CD4^+$ and $CD8^+$ T cells, natural killer cells, neutrophils, and infiltrating macrophages ($F4/80^{lo}CD11b^+$). With the exception of $CD8^+$ T cells, most liver immune cell subtypes, including infiltrating macrophages, significantly decreased in the setting of Treg augmentation with JES6-1/IL-2 (Figure 4B). Interestingly, the number of liver tissue–resident macrophages ($F4/80^{hi}CD11b^+$) significantly increased in response to JES6-1/IL-2. Additional characterization of the infiltrating and resident macrophage populations was performed to determine the functional effect of Treg augmentation on macrophages.

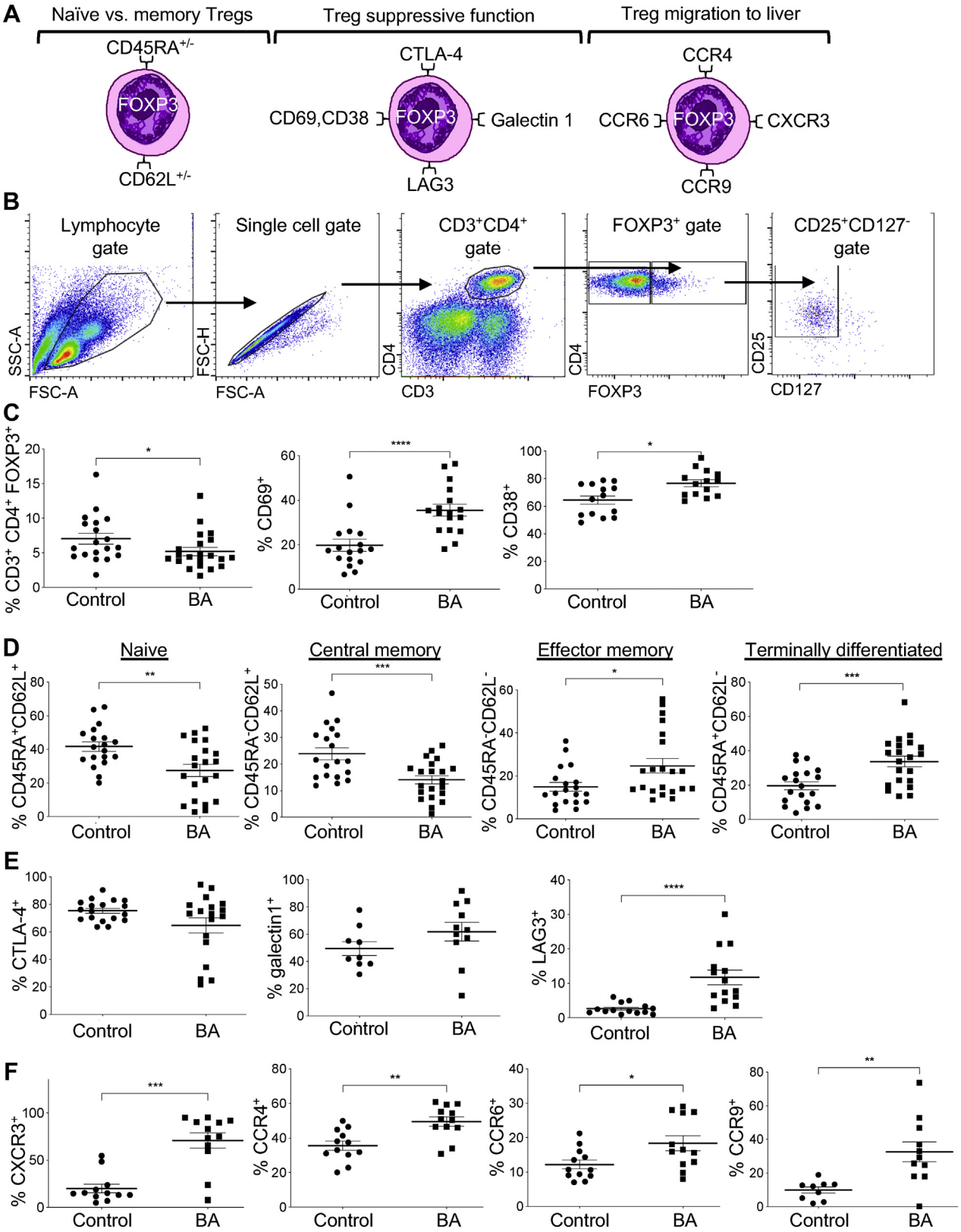

Figure 1. Activated peripheral blood Tregs lack upregulation of suppressive molecules in human BA. (A) Schematic of experimental analyses of peripheral blood Tregs; (B) Gating strategy for Treg cell surface flow cytometry analyses: sequential gating of lymphocyte population (FSC/SSC)– single cells– $CD3^{+}CD4^{+}$ T cells– $FoxP3^{+}$ Tregs– $CD25^{+}CD127^{-}$ Tregs; (C) Frequency of Tregs and percent of Tregs expressing activation markers CD69 and CD38; (D) Frequency of Treg maturation subsets; (E) Frequency of Treg proteins involved in suppression of inflammation; (F) Treg chemokine receptors involved in trafficking to the liver.

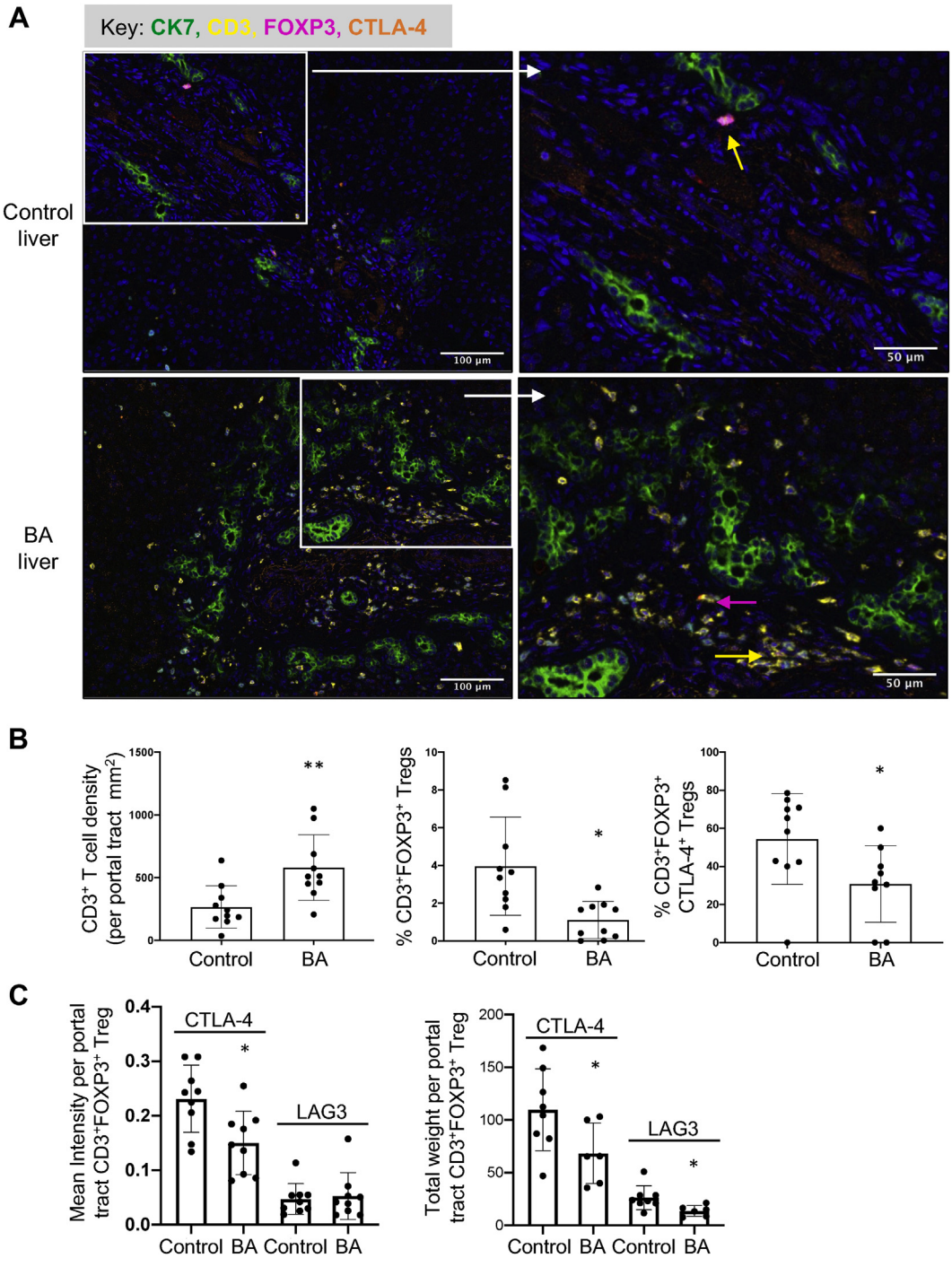

Figure 2. Deficits in human BA liver Treg frequency and Treg CTLA-4 expression. (A) A representative picture of control (top panel) and BA (lower panel) liver tissue stained for cytokeratin 7 (CK7; cholangiocyte), CD3 (T cell), FoxP3 (Treg), and CTLA-4 (suppressive molecule) using Vectra-6 immunohistochemistry. Yellow arrow: $CD3^{+}Foxp3^{+}$ Treg; pink arrow: $CD3^{+}FoxP3^{+}CTLA\text{-}4^{+}$ Treg; (B) Density of liver $CD3^{+}$ T cells per mm^2 and frequency of liver $CD3^{+}$ T cells that were $Foxp3^{+}$ and $FoxP3^{+}CTLA\text{-}4^{+}$; (C) Single-cell mean intensity and total weight of CTLA-4 and LAG3 expression on portal tract Tregs. *$P < .05$; **$P < .005$.

Treg Augmentation Impacts the Tissue-resident Macrophage Phenotype

Macrophages in the liver exert a wide variety of functions, including either proinflammatory tissue injury or anti-inflammatory tissue homeostasis. To that end, macrophages can be categorized as either proinflammatory (M1) or anti-inflammatory/immunosuppressive (M2).[21] Based on the changes observed in infiltrating and resident macrophages in response to Treg augmentation, we next determined if the infiltrating and resident macrophages were polarized to

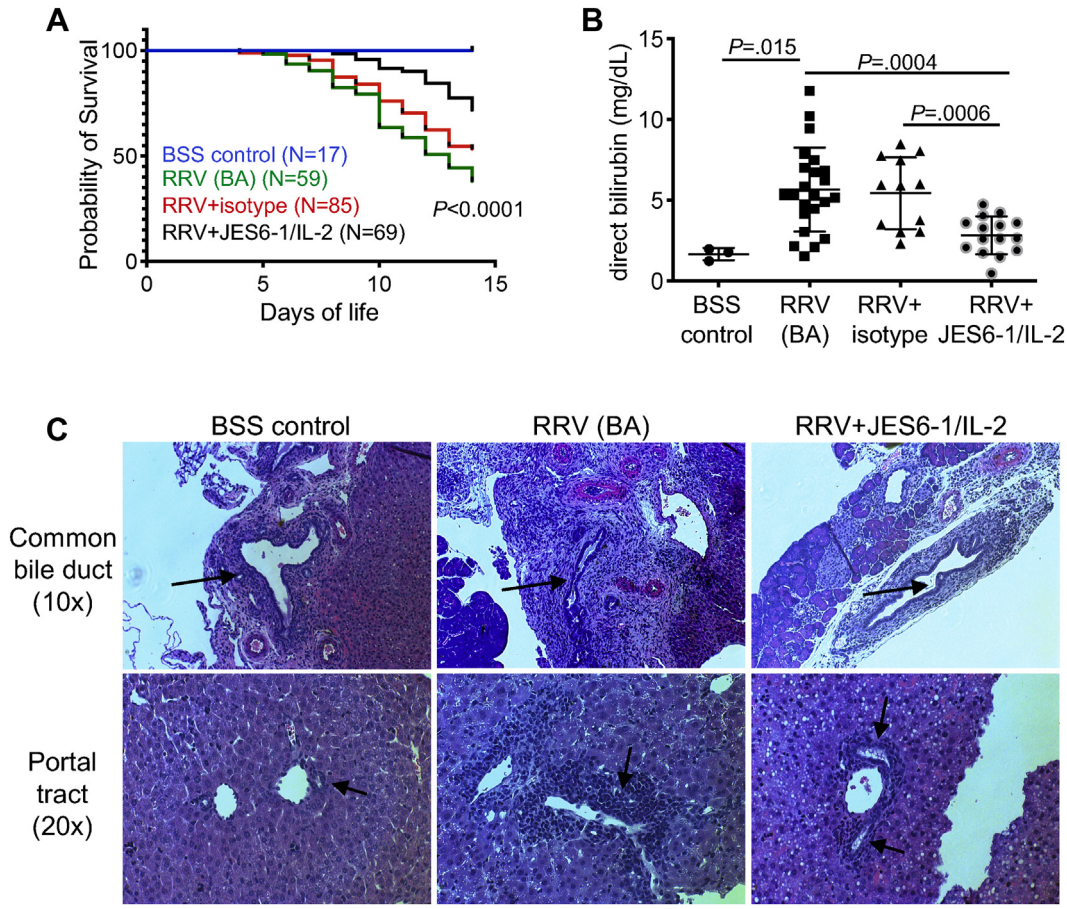

Figure 3. Treg augmentation therapy rescues from disease in the RRV-induced mouse model of BA. (A) Survival rates between groups; (B) serum direct bilirubin levels at DOL 14; (C) Representative H&E pictures of common bile duct and liver tissue at DOL 14; black arrow: bile ducts; [balanced salt solution (BSS), day of life (DOL), rhesus rotavirus (RRV)].

either an M1 or M2 phenotype. An important disclaimer is that macrophages can have a spectrum of activated phenotypes, rather than a discrete stable subpopulation, depending on the specific disease process.[22] Liver infiltrating and resident macrophages were isolated in high purity with a fluorescent-activated cell sorter based on CD11b and F4/80 expression (Figure 5A). Real-time PCR was used to characterize genes within the M1 (*Socs3*, *Il-6*, *Fpr2*, *Fabp4*) and M2 (*Arg1*, *Tgf-β*, *Timd4*) phenotypes.[22–24]

Verification of the liver M1 and M2 phenotypes in the normal (non-RRV infected) 14-day-old mouse revealed that infiltrating macrophages had increased amounts of M1 transcripts compared with resident macrophages and resident macrophages had higher levels of M2 transcripts than infiltrating macrophages (Figure 5B). In the diseased state, the RRV-infected BA mice resident macrophages revealed a dual functionality, with significantly increased expression of all M1 and M2 transcripts compared with BSS controls (Figure 5C). In the setting of Treg augmentation, all resident macrophage M1 markers significantly decreased; however, the M2 markers *Arg1* and *Tgf-β* also decreased with Treg augmentation (Figure 5C). The RRV-infected BA mice liver infiltrating macrophages had increased expression of M1 markers *Socs3* and *Fpr2* compared with BSS controls, and Treg augmentation significantly inhibited expression of these genes. No changes were found in infiltrating macrophage M2 markers in response to Treg augmentation.

Discussion

These investigations revealed that patients with BA have Treg deficiencies associated with lack of sufficient CTLA-4 expression that is necessary for cell-cell contact inhibition of inflammatory responses. Furthermore, Treg augmentation therapy in the murine model of BA protected from disease. This protection was associated with decreased liver inflammation, including significantly decreased infiltrating macrophages, concurrent with increased resident macrophages. The resident macrophages took on an inflammatory M1 phenotype in response to RRV infection (in addition to their baseline anti-inflammatory M2 phenotype). The M1 phenotype in both infiltrating and resident macrophages was inhibited with Treg augmentation therapy. Taken together, abnormal Treg suppressive function due to deficiencies in CTLA-4 results in biliary inflammation and injury that is abrogated by Treg augmentation.

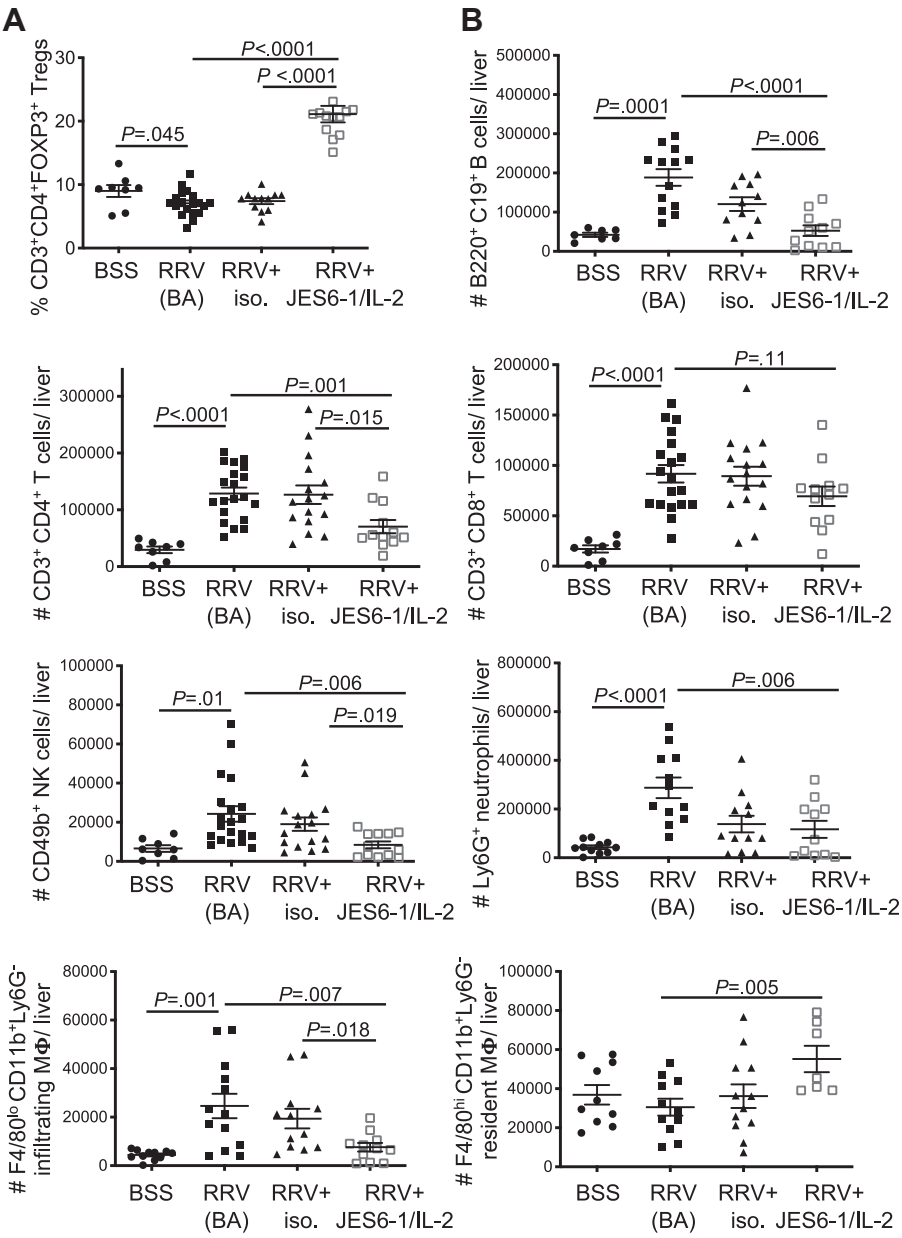

Figure 4. Treg augmentation therapy leads to decreased frequency of liver inflammatory cells in the RRV-induced mouse model of BA. (A) Flow cytometric analysis of liver Treg frequency; (B) Flow cytometric analyses of various liver immune cells (number of distinct immune cell type per whole mouse liver).

CTLA-4 is constitutively expressed on Tregs; on Treg activation, CTLA-4 is upregulated and functions as a negative immune regulator of T cell activation. CTLA-4–mediated Treg suppression is essential for the maintenance of peripheral tolerance and the prevention of T cell–mediated autoimmunity. Many autoimmune diseases are associated with defects in Tregs, including type I diabetes, inflammatory bowel disease, systemic lupus erythrocytosis, and CTLA-4 haploinsufficiency syndrome.[25] In BA, T cell autoimmunity targeting cholangiocytes contributes to disease pathogenesis.[1,3,4,14] Potential therapies that augment Treg function in humans include rapamycin (mTOR inhibitor)[26,27] and retinoic acid.[28,29] Furthermore, the CTLA-4-Fc fusion protein (abatacept) that mimics CTLA-4 function has been used to treat CTLA-4 haploinsufficiency.[30] There is a precedent for the use of Treg augmentation to treat autoimmune diseases in animal models as well. The original discovery of the Treg augmentation properties of JES6-1/IL-2 included the findings of protection from murine experimental autoimmune encephalomyelitis and tolerance of major histocompatibility complex-incompatible pancreatic islet cell transplants.[19] In a mouse model of sclerosing cholangitis, Treg augmentation with IL-2/anti–IL-2 immune complex resulted in resolution of biliary injury and fibrosis.[31] All these immunomodulators could be considered for future treatment trials in BA, to promote resolution of biliary inflammation and injury after Kasai portoenterostomy.

Augmentation of Tregs in murine BA resulted in inhibition of inflammatory-mediated biliary disease. The macrophage subsets were of particular interest, as the liver infiltrating macrophage numbers significantly decreased, concurrent with increased liver resident macrophages in response to Treg augmentation therapy. At baseline (noninfected mouse), the resident macrophages had an

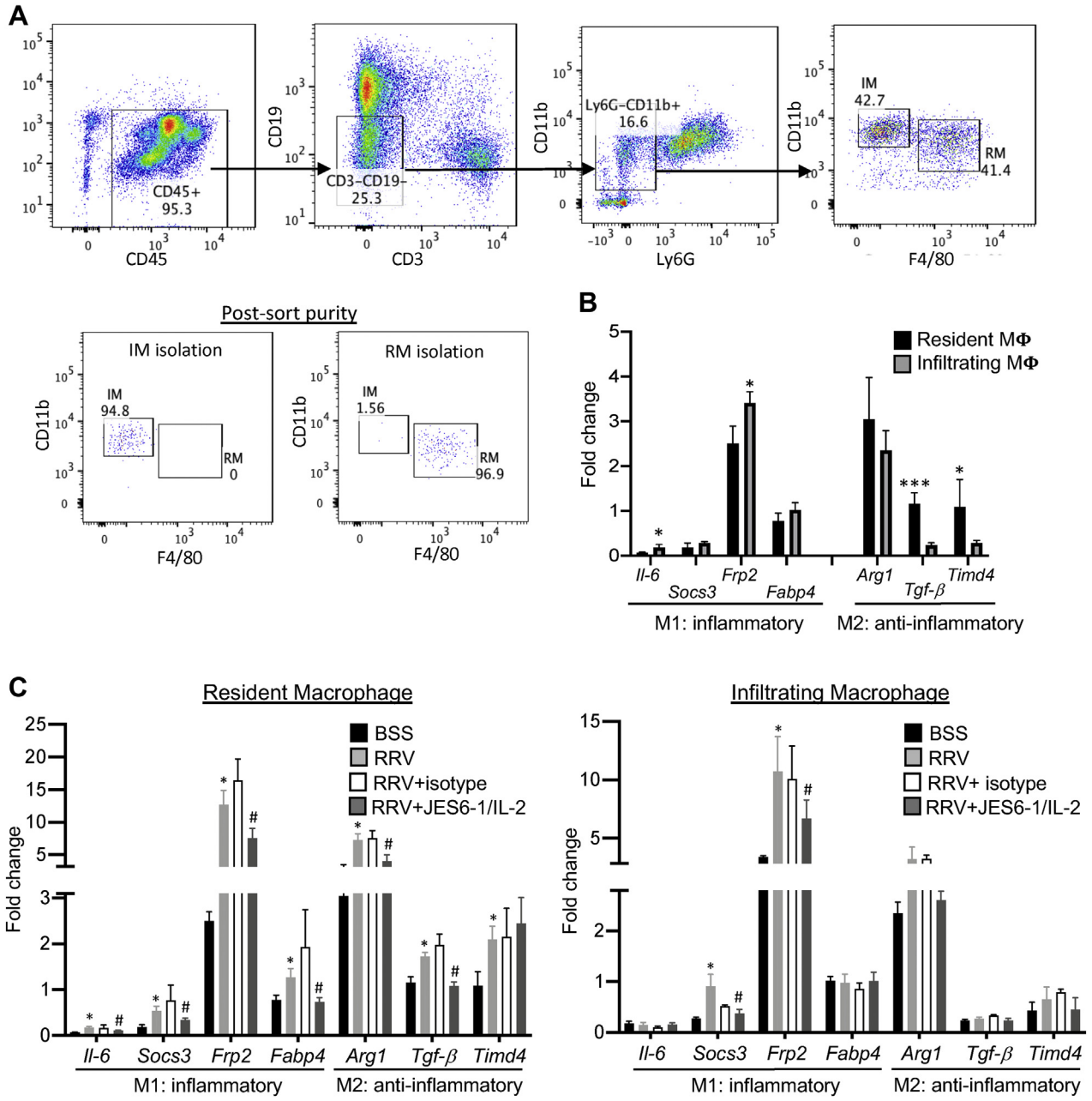

Figure 5. Phenotypes of liver infiltrating and resident macrophages based on mRNA expression. (A) Liver macrophage subsets [infiltrating macrophages (IM; F4/80^{lo}CD11b^{+}), tissue resident macrophages (RM; F4/80^{hi}CD11b^{+})] were isolated by flow cytometric cell sorting based on CD45^{+}CD3^{-}CD19^{-}Ly6G^{-} gating strategy. Post-sort purity check revealed ≥95% purity of sorted cell population that underwent subsequent RNA isolation. (B) Fold change mRNA expression of the macrophage inflammatory macrophage phenotype (M1) and suppressive macrophage phenotype (M2) in RM and IM from normal mouse livers (DOL 14); RM vs IM: $^{*}P < .05$; $^{***}P < .0005$; (C) Fold change of resident macrophage and infiltrating macrophage M1 and M2 genes; $^{*}P < .05$: BSS vs RRV, $^{\#}P < .05$: RRV vs JES6-1/IL-2.

anti-inflammatory M2 phenotype; on RRV infection, the resident macrophages took on a dual phenotype, with high expression of markers for both M1 and M2. Importantly, Treg augmentation inhibited the inflammatory M1 phenotype of resident macrophages. Recent investigations have focused on the role of Tregs in regulating and controlling innate immune responses, including altering macrophage subtypes and function.[32] In vitro studies of co-culture of Tregs and macrophages led to decreased human leukocyte antigen-DR isotype expression and proinflammatory cytokine production from macrophages.[33] Furthermore, Treg depletion led to exaggerated M1 macrophage activation in an animal model of endotoxic shock.[34] Pertinent to our study, there is known cross-talk between Tregs and regulatory M2 macrophages, as Tregs are able to direct macrophage differentiation to a M2 phenotype and play an important role in immune homeostasis.[32]

The importance of inflammatory (M1) macrophages to disease pathogenesis in BA has been recently described in both humans[35] and mice.[10] Novel strategies for therapeutic targeting of hepatic macrophages include agents that would dampen resident macrophage activation by influencing the gut-liver axis and inhibit recruitment of infiltrating macrophages to the liver, modulating macrophage polarization and augmenting M2 resident macrophages.[21] Future treatment trials for BA should include agents that enhance Treg number and/or function, mimic CTLA-4 function, and promote anti-inflammatory M2 macrophage phenotypes.

Materials and Methods

Human Biospecimens

Biospecimens were collected after parent/caretaker approval through the University of Colorado Institutional Review Board–approved study (#12-0069; Mack CL: PI). PBMCs were isolated from whole blood by Ficoll-gradient purification, placed in freezing media [10% dimethylsulfoxide, 90% fetal calf serum] and stored in liquid nitrogen until batch analyses. Formalin-fixed paraffin-embedded liver tissue was processed within the Children's Hospital Colorado Histology Laboratory, and tissue sections were acquired for IHC.

Flow Cytometry of Human PBMCs

PBMCs were incubated with 1% Fc block, followed by staining with the following fluorochrome-conjugated antibodies (clone): CD3 (UCHT1), CD4 (SK3), FOXP3 (206D), CD127 (A019DS), CD25 (M-A251), CD45RA (HI100), CD62L (DREG-56), CD69 (FN50), CD38 (HB-7), LAG3 (11C3C65), galectin1 (GAL1/1831), CTLA-4 (BSb-88), CCR4 (L291H4), CCR6 (G034E3), CCR9 (L053E8), and CXCR3 (G025H7). Cells were analyzed on a FACSCanto II flow cytometer, data were acquired using the FACSDiva software, and multiparameter flow cytometry data were analyzed using FlowJo software (BD, San José, CA). For human Treg PCR studies, cells were sorted using the FACS Aria flow cytometer, with >95% purity of the Treg subset ($CD45^{+}CD3^{+}CD4^{+}CD127^{lo}CD25^{+}$ cells).

Fluorescent IHC of Human Liver Tissue

Multispectral IHC analyses were performed using Vectra Automated Quantitative Pathology Systems (Akoya Biosciences) within the University of Colorado Human Immunology and Immunotherapy Initiative Core Facility. Slides were sequentially stained with antibodies specific for for CK7 (OV-TL 12/30, Agilent Dako) CD3 (LN10, Leica), CD8 (C8/144B, Agilent Technologies), FOXP3 (36A/E7, Abcam), CTLA-4 (BSb-88, Bio SB), and LAG3 (EPR4392(2), Abcam). Three to twenty portal track regions were chosen from each sample based on CK7 staining. For each region, 1600–4000 cells were selected for further analysis. Image analysis was performed using inForm software, version 2.4.10, (Akoya), including tissue segmentation, cell segmentation, and phenotyping to assign each cell to a phenotypic category. Further analysis was performed using R studio.

RRV-induced Mouse Model of BA

All mice were housed and handled through the UC Denver Office of Laboratory Animal Medicine (IACUC approval #040). BALB/c-FOXP3 GFP (C.Cg-$FoxP3^{tm2Tch}$/J) mice were purchased from infection-free colonies (Envigo Laboratories, Cambridgeshire, UK) and bred within the UC Denver animal facility. Mice were given a single intraperitoneal injection of 40 μl RRV (1.8×10^{6} pfu/mL) or BSS on DOL 1, followed by injection of either JES6-1 (25 μg)/IL-2 (1.5 μg) or isotype control (rat IgG2a, 25 μg), on DOL 4, 5, and 6. Mice were sacrificed on DOL 14, and pooled sera and tissues from 3 mice/pools were analyzed (3 pools = 9 mice/group/experiment and all experiments were performed 3 times). Results reflect the mean ± standard deviation of 3 separate experiments. Serum direct bilirubin was determined with kits from Diagnostic Chemicals Ltd (Charlottetown, Canada). Formalin-fixed paraffin-embedded liver and bile duct tissue was stained with hematoxylin-eosin. Digital photographs were obtained using the Olympus BX41 microscope (Melville, NY).

Mouse Liver Flow Cytometry and Cell Sorting

Tissue was homogenized with the Bellco Cellector tissue sieve (Vineland, NJ), and red cells were lysed with ACK buffer. Liver immune cells were enriched by Percoll gradient (40/60). Single-cell suspensions were incubated with Fc-block and stained with the following fluorochrome-conjugated antibodies (clone): CD45 (30-F11), CD3 (17A2), CD4 (RM4-5), CD8 (53–6.7), CD11b (M1/70), CD19 (6D5), F4/80 (BM8), Ly6G (1A8), Ly6C (HK1.4), CD19 (6D5), CD49b (DX5), NKG2D (191004), or isotype matched controls. Cells were visualized with the FACS LSR II flow cytometer (Becton-Dickinson, Mountain View, CA) using FlowJo software (Tree Star, Inc, Ashland, OR) for analysis. For mouse macrophage subset studies, cells were sorted using the FACS Aria flow cytometer (BD, San José, CA), with >95% purity of cell subsets.

Real-time PCR

Cellular RNA extraction was performed with the Trizol method, and RNA was purified using the Qiagen RNeasy kit (Valencia, CA). cDNA was synthesized from 2 μg of total RNA with the High-Capacity cDNA Reverse Transcription Kit (Thermo Fisher Scientific). Real-time PCR was performed using Power SYBR-Green PCR master mix (Thermo Fisher Scientific). qPCR was performed on a Bio-Rad C1000 touch thermal cycler real-time PCR system (Hercules, CA). Primer sequences are listed in Table A1.

Statistical Analysis

Values are expressed as mean ± standard deviation or standard error of the mean. One-way analysis of variance (ANOVA) with multiple comparisons was used when more than 2 groups were compared. The Student t-test for unpaired samples was used for comparison between 2 groups. The log-rank (Mantel-Cox) test was used for comparison of survival curves. PRISM Graph Pad software (La Jolla, CA) was used for statistical analyses. Differences in means were considered significant for P-values <.05. All authors had access to the study data and had reviewed and approved the final article.

Supplementary Materials

Material associated with this article can be found in the online version at https://doi.org/10.1016/j.gastha.2021.12.012.

References

1. Bezerra JA, Wells RG, Mack CL, et al. Biliary atresia: clinical and research challenges for the 21(st) century. Hepatology 2018;68:1163–1173.
2. Fanna M, Masson G, Capito C, et al. Management of biliary atresia in France 1986 to 2015: long-term results. J Pediatr Gastroenterol Nutr 2019;69:416–424.
3. Mack CL, Tucker RM, Lu BR, et al. Cellular and humoral autoimmunity directed at bile duct epithelia in murine biliary atresia. Hepatology 2006;44:1231–1239.
4. Mack CL, Falta MT, Sullivan AK, et al. Oligoclonal expansions of CD4+ and CD8+ T-cells in the target organ of patients with biliary atresia. Gastroenterology 2007;133:278–287.
5. Bednarek J, Traxinger B, Brigham D, et al. Cytokine-producing B cells promote immune-mediated bile duct injury in murine biliary atresia. Hepatology 2018;68:1890–1904.
6. Feldman AG, Tucker RM, Fenner EK, et al. B cell deficient mice are protected from biliary obstruction in the rotavirus-induced mouse model of biliary atresia. PLoS One 2013;8:e73644.
7. Yang L, Mizuochi T, Shivakumar P, et al. Regulation of epithelial injury and bile duct obstruction by NLRP3, IL-1R1 in experimental biliary atresia. J Hepatol 2018;69:1136–1144.
8. Shivakumar P, Mourya R, Bezerra JA. Perforin and granzymes work in synergy to mediate cholangiocyte injury in experimental biliary atresia. J Hepatol 2014;60:370–376.
9. Saxena V, Shivakumar P, Sabla G, et al. Dendritic cells regulate natural killer cell activation and epithelial injury in experimental biliary atresia. Sci Transl Med 2011;3:102ra94.
10. Lages CS, Simmons J, Maddox A, et al. The dendritic cell-T helper 17-macrophage axis controls cholangiocyte injury and disease progression in murine and human biliary atresia. Hepatology 2017;65:174–188.
11. Luo Y, Brigham D, Bednarek J, et al. Unique cholangiocyte-targeted IgM autoantibodies correlate with poor outcome in biliary atresia. Hepatology 2021;73:1855–1867.
12. Sakaguchi S. Naturally arising CD4+ regulatory t cells for immunologic self-tolerance and negative control of immune responses. Annu Rev Immunol 2004;22:531–562.
13. Tucker RM, Feldman AG, Fenner EK, et al. Regulatory T cells inhibit Th1 cell-mediated bile duct injury in murine biliary atresia. J Hepatol 2013;59:790–796.
14. Lages CS, Simmons J, Chougnet CA, et al. Regulatory T cells control the CD8 adaptive immune response at the time of ductal obstruction in experimental biliary atresia. Hepatology 2012;56:219–227.
15. Miethke AG, Saxena V, Shivakumar P, et al. Post-natal paucity of regulatory T cells and control of NK cell activation in experimental biliary atresia. J Hepatol 2010;52:718–726.
16. Brindley SM, Lanham AM, Karrer FM, et al. Cytomegalovirus-specific T-cell reactivity in biliary atresia at the time of diagnosis is associated with deficits in regulatory T cells. Hepatology 2012;55:1130–1138.
17. Yang Y, Liu YJ, Tang ST, et al. Elevated Th17 cells accompanied by decreased regulatory T cells and cytokine environment in infants with biliary atresia. Pediatr Surg Int 2013;29:1249–1260.
18. Kim S, Moore J, Alonso E, et al. Correlation of immune markers with outcomes in biliary atresia following intravenous immunoglobulin therapy. Hepatol Commun 2019;3:685–696.
19. Webster KE, Walters S, Kohler RE, et al. In vivo expansion of T reg cells with IL-2-mAb complexes: induction of resistance to EAE and long-term acceptance of islet allografts without immunosuppression. J Exp Med 2009;206:751–760.
20. Boyman O, Kovar M, Rubinstein MP, et al. Selective stimulation of T cell subsets with antibody-cytokine immune complexes. Science 2006;311:1924–1927.
21. Ju C, Tacke F. Hepatic macrophages in homeostasis and liver diseases: from pathogenesis to novel therapeutic strategies. Cell Mol Immunol 2016;13:316–327.
22. Murray PJ, Wynn TA. Protective and pathogenic functions of macrophage subsets. Nat Rev Immunol 2011;11:723–737.
23. Jablonski KA, Amici SA, Webb LM, et al. Novel markers to delineate murine M1 and M2 macrophages. PLoS One 2015;10:e0145342.
24. Klopfleisch R. Macrophage reaction against biomaterials in the mouse model - phenotypes, functions and markers. Acta Biomater 2016;43:3–13.
25. Mitsuiki N, Schwab C, Grimbacher B. What did we learn from CTLA-4 insufficiency on the human immune system? Immunol Rev 2019;287:33–49.
26. Ogino H, Nakamura K, Iwasa T, et al. Regulatory T cells expanded by rapamycin in vitro suppress colitis in an experimental mouse model. J Gastroenterol 2012;47:366–376.
27. Esposito M, Ruffini F, Bellone M, et al. Rapamycin inhibits relapsing experimental autoimmune encephalomyelitis by both effector and regulatory T cells modulation. J Neuroimmunol 2010;220:52–63.
28. Bai A, Lu N, Guo Y, et al. All-trans retinoic acid down-regulates inflammatory responses by shifting the Treg/Th17 profile in human ulcerative and murine colitis. J Leukoc Biol 2009;86:959–969.
29. Van YH, Lee WH, Ortiz S, et al. All-trans retinoic acid inhibits type 1 diabetes by T regulatory (Treg)-dependent suppression of interferon-gamma-producing T-cells without affecting Th17 cells. Diabetes 2009;58:146–155.
30. Lanz AL, Riester M, Peters P, et al. Abatacept for treatment-refractory pediatric CTLA4-haploinsufficiency. Clin Immunol 2021;229:108779.
31. Taylor AE, Carey AN, Kudira R, et al. Interleukin 2 promotes hepatic regulatory T cell responses and protects from biliary fibrosis in murine sclerosing cholangitis. Hepatology 2018;68:1905–1921.

32. Okeke EB, Uzonna JE. The pivotal role of regulatory T cells in the regulation of innate immune cells. Front Immunol 2019;10:680.
33. Tiemessen MM, Jagger AL, Evans HG, et al. CD4+CD25+Foxp3+ regulatory T cells induce alternative activation of human monocytes/macrophages. Proc Natl Acad Sci U S A 2007;104:19446–19451.
34. Okeke EB, Okwor I, Uzonna JE. Regulatory T cells restrain CD4+ T cells from causing unregulated immune activation and hypersensitivity to lipopolysaccharide challenge. J Immunol 2014;193:655–662.
35. Taylor SA, Chen SY, Gadhvi G, et al. Transcriptional profiling of pediatric cholestatic livers identifies three distinct macrophage populations. PLoS One 2021;16:e0244743.

Received December 3, 2021. Accepted December 22, 2021.

Correspondence:
Address correspondence to: Cara L. Mack, MD, Professor of Pediatrics, Section of Gastroenterology, Hepatology & Nutrition, Department of Pediatrics, Children's Hospital Colorado, University of Colorado School of Medicine, 13123 E 16th Ave., B290, Aurora, Clorado 80111. e-mail: cara.mack@childrenscolorado.org.

Authors' Contributions:
Yuhuan Luo and Joseph Bednarek contributed to data collection, data analyses, and manuscript writing/editing. Alexander Chaidez contributed to data collection and manuscript editing. Dong Wang contributed to data analyses and manuscript editing. Shaikh Atif contributed to design of study, data analyses, and manuscript editing. Cara L. Mack contributed to design of study, data analyses, and manuscript writing/editing.

Conflicts of Interest:
The authors disclose no conflicts.

Funding:
The study was funded by North American Society of Pediatric Gastroenterology, Hepatology and Nutrition Foundation/Takeda Pharmaceutical Products Inc Research Innovation Award. It received core support from University of Colorado Human Immunology and Immunotherapy Initiative.

Ethical Statement:
The corresponding author, on behalf of all authors, jointly and severally, certifies that their institution has approved the protocol for any investigation involving humans or animals and that all experimentation was conducted in conformity with ethical and humane principles of research.

Data Transparency Statement:
Data and analytic methods will be available on individual researcher request; however, study materials will not be available to other researchers.